Probing the photosensitizing and inhibitory effects of dissolved organic matter by using *N,N*-dimethyl-4-cyanoaniline (DMABN)

Frank Leresche,[†, ‡] Urs von Gunten [†, ‡, ♯] and Silvio Canonica[†, *]

[†]Eawag, Swiss Federal Institute of Aquatic Science and Technology, Überlandstrasse 133, CH-8600 Dübendorf, Switzerland

[‡]School of Architecture, Civil and Environmental Engineering (ENAC), Ecole Polytechnique Fédérale de Lausanne (EPFL), CH-1015 Lausanne, Switzerland

[♯]Institute of Biogeochemistry and Pollutant Dynamics, ETH Zürich, Universitätstrasse 16, CH-8092, Zürich, Switzerland

This document is the accepted manuscript version of the following article:
Leresche, F., Von Gunten, U., & Canonica, S. (2016). Probing the photosensitizing and inhibitory effects of dissolved organic matter by using N,N-dimethyl-4-cyanoaniline (DMABN). Environmental Science and Technology, 50(20), 10997-11007. https://doi.org/10.1021/acs.est.6b02868

ABSTRACT

Dissolved organic matter (DOM) can act as a photosensitizer and an inhibitor in the phototransformation of several nitrogen-containing organic contaminants in surface waters. The present study was performed to select a probe molecule that is suitable to measure these antagonistic properties of DOM. Out of nine studied nitrogen-containing aromatic compounds, 4-cyanoaniline, *N*,*N*-dimethyl-4-cyanoaniline (DMABN), sotalol (a β-blocker) and sulfadiazine (a sulfonamide antibiotic) exhibited a marked photosensitized transformation that could be substantially inhibited by addition of phenol as a model antioxidant. The photosensitized transformation of DMABN, the selected probe compound, was characterized in detail under UV-A and visible irradiation ($\lambda > 320$ nm) to avoid direct phototransformation. Low reactivity of DMABN with singlet oxygen was found (second-order rate constant $<2\times10^7$ $M^{-1}s^{-1}$). Typically at least 85% of the reactivity of DMABN could be inhibited by DOM or the model antioxidant phenol. The photosensitized transformation of DMABN mainly proceeded (>72%) through demethylation yielding *N*-methyl-4-cyanoaniline and formaldehyde as primary products. In solutions of standard DOM extracts and their mixtures the phototransformation rate constant of DMABN was shown to vary non-linearly with DOM concentration. Model equations describing the dependence of such rate constants on DOM and model antioxidant concentrations were successfully used to fit experimental data.

TOC/Abstract Art

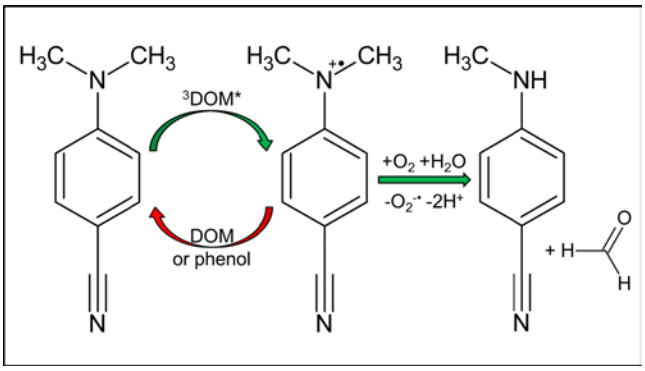

INTRODUCTION

Contaminants with electron-rich moieties in their molecular structure are susceptible to light-induced oxidation reactions in the aquatic environment. Experimental evidence accumulated during the last two decades points at excited triplet states of the dissolved organic matter (DOM) as key photooxidants responsible for these reactions. The contaminants that have been shown so far to react with excited triplet DOM ($^3DOM^*$) and presumably undergo oxidative transformation comprise many compounds with phenolic or aniline moieties. They include phenols with simple electron-donating substituents,[1] bisphenol A,[2] phenolic phytoestrogens,[3, 4] ring- or *N*-substituted anilines,[5, 6] sulfonamide antibiotics,[6-8] aminopyrimidine antibiotics,[9, 10] phenylurea herbicides,[11] and further pesticides.[12] Model photosensitizers were used to mimick DOM chromophores that can generate oxidizing $^3DOM^*$ upon photoexcitation, and laser flash photolysis studies with such photosensitizers were performed to further clarify the nature of the reaction between oxidizing $^3DOM^*$ and various substrates in aqueous solution.[13-15] Second-order rate constants for the quenching of the excited triplet state of selected aromatic ketones by a series of substituted phenols were rationalized in terms of a one-electron transfer.[13] An analogous conclusion was drawn for the quenching of excited triplet methylene blue by substituted anilines.[15] However, the latter triplet state appeared to react through a proton-coupled electron transfer with substituted phenols.[15]

The radicals formed after the initial oxidation step, such as aniline radical cations, are relatively strong one-electron oxidants (standard reduction potentials of ≈1.0±0.2 V vs. NHE for a series of *para*-substituted aniline radical cations[16]). Nevertheless they may lose a proton, which leads to a significant loss in oxidative strength. The radical cations or their deprotonated counterparts can

59 further react to yield stable transformation products, as can be deduced from the observed
60 depletion of parent compound in photoirradiated samples (see the aforementioned examples of
61 contaminants). It has been postulated that oxidation intermediates of the substrate, but primarily
62 the radical cations, may react with electron-rich moieties in the DOM, leading to reformation of
63 the substrate.[6] This hypothesis was put forward to explain the decrease in depletion rate
64 constants observed for several aromatic contaminants and model compounds, particularly those
65 containing aromatic amino groups, in steady-state irradiation experiments.[6, 17] This effect has
66 been referred to as "inhibition of triplet-induced oxidation (or transformation)" and shown to
67 also occur in model systems in which DOM had been replaced by phenols, either unsubstituted
68 or bearing electron-donating substituents.[18] Recently, for partially oxidized humic substances a
69 good correlation was found between the electron donating capacity (EDC) and the inhibitory
70 effect on triplet-induced oxidation,[19] which corroborates the idea that antioxidant moieties of the
71 DOM, in particular phenolic components, are responsible for the inhibition of triplet-induced
72 oxidation.

73 The concept of inhibition of transformation as described above has been used to date to
74 understand and describe the rates of direct and indirect phototransformations in surface waters-
75 like conditions.[20, 21] The present study was conceived to further develop the application of this
76 concept to DOM-induced indirect phototransformations in surface waters. We primarily aimed at
77 selecting a model compound that may be employed as a probe to assess the inhibition of triplet-
78 induced oxidation in natural waters. In the first part of the study, several organic compounds
79 were photoirradiated in aqueous solutions containing DOM, with or without the addition of
80 phenol as an antioxidant, to evaluate their suitability as model compounds. One of these
81 compounds, namely *N*,*N*-dimethyl-4-cyanoaniline (abbreviated as DMABN from the alternative

name 4-dimethylaminobenzonitrile) was selected and further investigated to characterize its direct and indirect phototransformation pathways. These investigations included the assessment of the role of singlet oxygen in the indirect phototransformation, the identification of the main reaction products as well as the measurements of the phototransformation rate constants of DMABN in aqueous solutions of DOM mixtures and surface water mixtures.

MATERIALS AND METHODS

Chemicals and Solutions. All chemicals were commercially available and used as received. A complete list of chemicals is given in the Supporting Information (SI), Text S1. All solutions were made in ultrapure water (resistivity 18.2 MΩ cm) obtained from a Barnstead Nanopure® purification system. Stock solutions of target compounds (~500 μM) were kept in the dark at 4 °C. Suwannee River fulvic acid (SRFA, catalogue number 1S101F) and Pony Lake fulvic acid (PLFA, 1R109F) were purchased from the International Humic Substances Society (IHSS, St. Paul, Minnesota). Stock solutions of the fulvic acids were prepared at a concentration of ~50 $mg_C\ L^{-1}$. The concentration of the first stock solutions of PLFA and SRFA was quantified by total organic carbon (TOC) analysis, while the concentration of subsequent stock solutions was determined spectrophotometrically using the first two stock solutions as references. Full characteristics of the fulvic acids are given in the SI, Table S1 and Figure S1.

Natural Waters. Natural water samples were taken on November 18th, 2014 from the outlet of Lake Greifensee (GW) (47.3727 N, 8.6557 E), a small eutrophic lake in northern Switzerland described in detail elsewhere,[22] and on November 14th, 2014 near the outlet of Etang de la Gruère (EG) (47.2376 N, 7.0494 E), a small pond surrounded by timbers and boggy wetland

(surface area ~30'000 m^2). Waters were filtered on pre-washed 0.45 µm pore size cellulose nitrate filters and stored in the dark at 4 °C. GW had a rather low DOM concentration (3.3 mg_C L^{-1}) and pH 8.3, while EG was high in DOM concentration (22.8 mg_C L^{-1}) with a pH of 7.7 (see SI, Table S2 and Figure S2 for more physicochemical parameters).

Irradiation Experiments. Irradiations were performed using either a solar simulator (Heraeus model Suntest CPS$^+$) or a merry-go-round photoreactor (DEMA model 125, Hans Mangels, Bornheim-Roisdorf, Germany) equipped with a medium-pressure mercury lamp and a borosilicate glass cooling jacket. A detailed description of the irradiation equipment is available elsewhere.[1, 23, 24] The merry-go-round photoreactor (see sketch in the SI, Figure S3) was operated using two different setups. For irradiations of solutions containing DOM as a photosensitizer, a Heraeus Noblelight medium-pressure Hg lamp, model TQ 718, operated at 500 W, and a 0.15 M sodium nitrate filter solution were used, whereby irradiation wavelengths <320 nm were cut-off. Experiments with rose Bengal (RB) as a photosensitizer were done using a Heraeus Noblelight medium pressure Hg lamp, model TQ 150, operated at 150 W and a filter solution containing 0.25 M sodium nitrate and 0.05 M sodium nitrite, whereby irradiation wavelengths <370 nm were cut-off. In addition, for the latter experiments the cooling jacket was wrapped with two stainless steel wire cloths to reduce irradiance by a factor of ≈6. The spectral distributions of the light sources in the wavelength range of 250–450 nm (see SI, Figure S4) were measured using a calibrated spectroradiometer system model ILT950-UV (International Light Technologies, Peabody, MA, U.S.A.). The photon fluence rate, measured by chemical actinometry using an aqueous solution of *p*-nitroanisole (10 µM) and pyridine (600 µM) according to a well-established procedure[25] (see SI, Text S2 and Table S3), was determined to be 165 (±15%) µE m^{-2} s^{-1} for the solar simulator in the 290–400 nm range. This value is representative for conditions

found at the surface of a natural water at midday of a clear-sky day between summer and autumn at 40° N latitude.[20]

Aqueous samples containing 5 μM of a single target compound, variable concentrations of DOM and, except for natural waters, 5 mM phosphate buffer (final solution pH 8.0) were irradiated at 25±1 °C in glass-stoppered quartz tubes (internal diameter 15 mm, external diameter 18 mm). The presence and concentration of additional components, such as phenol and individual photosensitizers or scavengers, is specified when discussing the results of the corresponding experiments. In the experiments using a mixture of GW and EG waters, the pH of GW was adjusted to the pH of EG using small amounts of hydrochloric acid (0.03M). Aliquot samples of 400 μL were taken at regular time intervals during the irradiation experiments.

Analytical Instrumentation. Total organic carbon analyses of solutions and water samples were done using a Shimadzu TOC-L CSH total organic carbon (TOC) analyzer. The concentration of target compounds (including furfuryl alcohol), phenol and the reaction product *N*-methyl-4-cyanoaniline were determined using high-performance liquid chromatography (HPLC). A complete description of the HPLC system and methods is given in the SI, Text S3 and Table S4. Electronic absorption spectra were recorded using an Agilent Cary 100 UV-Vis spectrophotometer. A Metrohm model 632 pH meter equipped with a Thermo scientific pH electrode (model Orion 8115SC) and a Metrohm model 712 conductometer were employed to measure pH and conductivity, respectively. Formaldehyde was quantified using the Hantzsch colorimetric titration method[26, 27] following the experimental details given in the SI, Text S4.

Determination of Rate Constants and Model Parameters. Pseudo-first-order phototransformation rate constants, k_{TC}^{obs} (s^{-1}), for a given target compound (TC) were obtained

by linear regression of its natural logarithmic relative residual concentration over irradiation time *t*, according to the following relationship:

$$\ln\left(\frac{[TC]_t}{[TC]_0}\right) = -k_{TC}^{obs} t \,. \qquad (1)$$

For merry-go-round irradiation experiments these rate constants were corrected for light screening caused by DOM, as described in the SI, Text S5. In the case of experiments performed in the presence of high phenol concentration, excited triplet quenching by phenol was included in the correction as described in the SI, Text S6. Rate constants for experiments conducted using RB as a photosensitizer were calculated according to the special procedure described in the SI, Text S7, which takes partial degradation of RB during irradiation into account. All corrected rate constants are termed as $k_{TC}^{obs,c}$. All data fits to non-linear model equations were performed using the software Origin, version 8.0 (Origin Lab) by applying the Levenberg-Marquardt minimization algorithm.

RESULTS AND DISCUSSION

Screening Study on Selected Compounds Using Simulated Sunlight.

Selection of Compounds. Nine compounds (for chemical structures see SI, Figure S6) were selected to perform the first, exploratory part of the study. The compounds were chosen among possible candidates satisfying the following conditions: (1) Triplet-induced oxidation was known or expected to play a substantial role in their transformation under sunlight in surface waters; (2) Inhibition of triplet-induced oxidation by DOM or model antioxidants was known or expected.

169 The first criterion applies to many actual organic contaminants and model compounds that are
170 prone to oxidation (e.g., phenol and aniline derivatives, see *Introduction* section for a more
171 detailed list) and for which the direct phototransformation is of minor relevance. The second
172 criterion mainly applies to aromatic amines. Five of the selected compounds were substituted
173 anilines: 4-Cyanoaniline, 4-*N*,*N*-dimethylcyanoaniline (both model compounds) and
174 4-aminobenzoic acid (a sunscreen agent), and in addition the two sulfonamide antibiotics
175 sulfadiazine and sulfadimethoxine. Two aminopyrimidine derivatives used as antibiotics, namely
176 trimethoprim and ormethoprim were also selected as representatives of heteroaromatic amines.
177 Finally, the two β-blockers propranolol (a 2-naphthol derivative) and sotalol (a sulfonamide
178 derivative) were selected to check if naphthol and sulfonamide functionalities also undergo
179 inhibition of triplet-induced oxidation by DOM.

180 *Phototransformation Experiments.* The phototransformation kinetics of each selected compound
181 dissolved in buffered ultrapure water, in slightly diluted natural water (GW 90%/ultrapure water
182 10% (vol/vol)), and in PLFA or SRFA solutions (5 mg_C L^{-1}, pH8) was studied under simulated
183 sunlight. For each compound, four additional samples of the same composition as
184 aforementioned but amended with phenol (10 μM final concentration) were also investigated to
185 assess a possible inhibition of transformation caused by this model antioxidant. Pseudo-first-
186 order phototransformation rate constants for all compounds and solution compositions are
187 represented in Figure 1. Rate constants for phototransformation in ultrapure water solution,
188 which was assumed to represent direct phototransformation, were lower than overall
189 phototransformation rate constants in the presence of DOM for many of the studied compounds.
190 The electronic absorption spectra of the compounds (see SI, Figure S6) significantly overlap with
191 the emission spectrum of the solar simulator (see SI, Figure S4). Values of the direct

phototransformation quantum yields, determined as described elsewhere,[20] are displayed in Figure 1 and collected together with the phototransformation rate constants in Table S6 of the SI. They are generally on the order of 10^{-3} mol einstein^{-1} except for sotalol, which has by far the highest value of about 0.2 mol einstein^{-1}. This explains why, although the absorption spectrum of sotalol has a very small overlap with the spectrum of the solar simulator, its direct phototransformation rate constant was rather high.

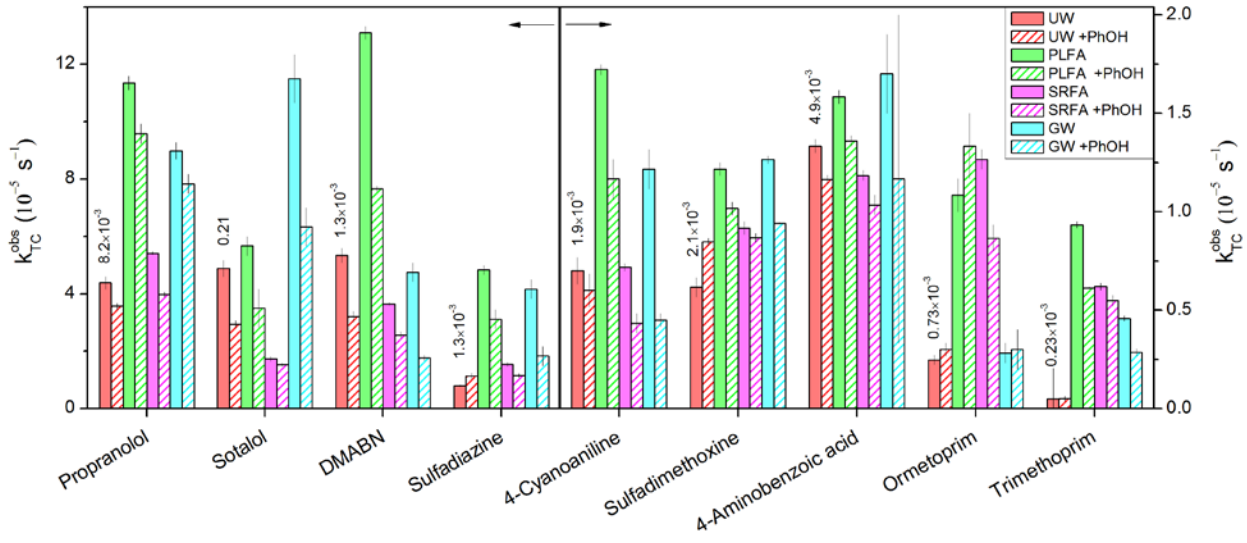

Figure 1. Phototransformation rate constants of the investigated compounds under simulated sunlight (λ > 290 nm). Bar colors designation (from left to right): Red for ultrapure water (UW, the quantum yield for direct phototransformation is given above the bar), green for Pony Lake fulvic acid (PLFA, 5.0 mg_C L^{-1}), magenta for Suwannee River fulvic acid (SRFA, 5.0 mg_C L^{-1}), and blue for 90% (vol) lake Greifensee water (GW, 3.0 mg_C L^{-1}). Fully colored and hatched bars represent data from experiments conducted in the absence and presence of 10 µM phenol (PhOH), respectively. Error bars represent standard errors obtained from linear regression. Note

211 the scale magnification on the right y-axis of the diagram for the compounds with lower
212 photoreactivity.

213

214 The presence of DOM affected in most cases the phototransformation rate constants in
215 comparison to buffered pure water solutions, except for 4-aminobenzoic acid, for which no
216 significant effect was observed. However, the effect depended strongly on the type of DOM. In
217 PLFA solutions and lake water (GW), a substantial increase in phototransformation rate
218 constants with respect to ultrapure water was often observed. For SRFA such an increase was
219 less prominent, and in some cases (sotalol, DMABN) even a decrease of the rate constant was
220 observed.

221 Addition of phenol caused a marked reduction in phototransformation rate constants in PLFA
222 and GW solution for the following compounds: sotalol, DMABN, sulfadiazine, 4-cyanoaniline
223 and trimethoprim. In SRFA solution, addition of phenol caused a less important reduction in the
224 photodegradation rate constants of these four compounds. A clear reduction of direct
225 phototransformation rate constants (UW results) was observed only for sotalol and DMABN. A
226 compound-specific discussion of the results from Figure 1 is given in the following.

227 *Propranolol.* This readily photoreactive β-blocker undergoes both direct[28, 29] and indirect
228 phototransformation,[30] the latter probably due to $^3DOM^*$.[30] The rather small reduction of
229 photoreactivity observed upon phenol addition makes it a weak indicator of the inhibitory effect.
230 Moreover, the positive charge present on the protonated amino group at circumneutral pH (pK_a =
231 9.5[31]) favors the association of propranolol with DOM due to electrostatic attraction, and this
232 could complicate its use as a model compound.

Sotalol. The photoreactivity pattern of sotalol is peculiar, because almost no photosensitization by PLFA could be observed, while SRFA strongly reduced the phototransformation rate constant with respect to UW. In contrast, an important enhancement of the rate constant was observed for GW, but the reason of this effect is unclear. This complex behavior hinders the use of sotalol as a model compound. The strong reduction of the phototransformation rate constants observed upon phenol addition indicates a possible role of DOM as an inhibitor, which should be considered in future studies on the phototransformation of sotalol.

DMABN. This compound exhibits the highest phototransformation rate constants among the investigated compounds in UW and PLFA solutions. The addition of phenol causes an important inhibitory effect, which is more pronounced in PLFA and GW solution than in SRFA solution. This behavior is similar to the one already observed for sulfadiazine and for sulfamethoxazole (for the latter compound regarding irradiation performed under UV-A) and extensively discussed in terms of the differential photosensitizing and inhibitory properties of the various DOMs.[20] Thus, DMABN appears to be a favorable model compound.

Sulfadiazine. The present results on this sulfonamide antibiotic are in agreement with data from previous studies,[6, 18, 20] which show the potential of this compound as a probe for the photosensitizing and inhibitory effects of DOM.

4-Cyanoaniline. The photoreactivity pattern of 4-cyanoaniline, including the effect of phenol addition, is similar to DMABN, its *N*,*N*-dimethylated derivative, but the absolute phototransformation rate constants are smaller by a factor of ≈4. Because of a less efficient phototransformation, it is less adequate than DMABN as a model compound.

Sulfadimethoxine. The phototransformation of sulfadimethoxine is enhanced at variable extents by the presence of DOM, in agreement with a previous study.[8] However, addition of phenol leads to a small reduction in phototransformation in the presence of DOM, while a small increase is observed for UW solution. This small and ambiguous effect of phenol as well as the relatively slow phototransformation hinder the use of sulfadimethoxine as a convenient model compound.

4-Aminobenzoic acid. The direct phototransformation of this aniline appears to be the dominant mechanism. The absence of significant inhibition upon phenol addition makes this compound inadequate for the sake of the present study.

Ormetoprim. Indirect phototransformation appeared to be dominant in PLFA and SRFA solutions, but no inhibition effect upon phenol addition could be observed for this antibiotic, Due to the high structural similarity to trimethoprim, we refer to the following discussion regarding the possible phototransformation mechanisms.

Trimethoprim. The photoreactivity of trimethoprim, which is very low in UW, is highly enhanced by DOM, and the inhibitory effect of phenol is important. However, the rate constants are quite low. Previous experiments performed using the model photosensitizers 4-carboxybenzophenone (CBBP) and 2-acetonaphthone (2AN)[6, 17] showed that trimethoprim was highly reactive with triplet CBBP, which has a high one-electron reduction potential (1.83 V vs. NHE, calculated from data given elsewhere[32]) but reacted very slowly in the presence of 2AN, for which the reduction potential was calculated to be much lower (1.34 V vs. NHE). The low photoreactivity of trimethoprim, which is the main drawback against its use as a model compound, may thus be rationalized considering that $^3DOM^*$ has an intermediate reduction potential compared to the excited triplet states of the model ketones.

Final Selection. Based on the aforementioned considerations we selected DMABN as the best-suited probe compound to be employed to explore the dual role of DOM as a photosensitizer and inhibitor of triplet-induced phototransformations. The main advantages of DMABN with respect to the other studied compounds are related to (a) a fast phototransformation and (b) an important inhibitory effect of phenol on the phototransformation. All potential probe compounds except trimethoprim (which was considered to be unsuited as a probe compound) exhibited a relatively important direct phototransformation under simulated sunlight. This drawback may be eliminated by using alternative UV irradiation conditions (λ>320 nm) which reduce the absorption rates by the probe compound itself. As will be shown in the following sub-sections, merry-go-round irradiation conditions with λ>320 nm turned out to be very appropriate for investigating DMABN. A further advantage of DMABN is its relatively simple molecular structure with absence of electric charge at circumneutral pH, and existing information about transient excited and radical species,[33] which are expected to facilitate mechanistic studies.

Characterization of the Indirect Phototransformation of DMABN in the Presence of DOM. Photoirradiation of sample solutions was performed in this part of the study using the merry-go-round photoreactor setup with emission wavelength > 320 nm, a setup that has proven valuable in a number of previous studies.[1, 14, 20]

Estimation of the contribution of singlet oxygen and hydroxyl radical to the photosensitized transformation of DMABN. A high selectivity for a direct oxidation reaction by $^3DOM^*$ is a basic condition that a model compound should fulfill within the objective of the present study. Therefore, it is central to characterize and quantify possible photoinduced side reactions of DMABN in the presence of DOM. An important photooxidant that is always present during

DOM photosensitization is singlet (molecular) oxygen ($^1\Delta_g$), a reactive oxygen species that gives rise to photooxidations and photooxygenations of organic compounds in a highly selective manner.[34] The contribution of singlet oxygen to the phototransformation of DMABN was estimated by performing various irradiation experiments (see Table 1) comprising the addition of a selective singlet oxygen quencher (sodium azide, NaN_3), the use of heavy water as a solvent to increase the steady-state concentration of singlet oxygen by an order of magnitude,[35] the application of RB as a selective photosensitizer for the production of singlet oxygen,[36] and the use of furfuryl alcohol as a selective singlet oxygen probe compound.[37] For a detailed discussion of the rate constants given in Table 1 we refer to the SI, Text S10. Overall, the rate constants for the phototransformation of DMABN are only marginally affected by the presence of singlet oxygen quenchers or enhancers, even in the presence of RB as the photosensitizer. The maximum second-order rate constant for the reaction of DMABN with singlet oxygen was estimated to be 1.9×10^7 M^{-1} s^{-1} (from H_2O experiments) or 1.3×10^6 M^{-1} s^{-1} (from D_2O experiments). Also, the fractional contribution of singlet oxygen to the transformation of DMABN photosensitized by PLFA (5 mg_C L^{-1}) was estimated to be lower than 5%. Additional experiments using 2-propanol (10 mM) as a hydroxyl radical scavenger confirmed that this reactive species had a negligible contribution to the transformation of DMABN in PLFA solutions.

Table 1. Phototransformation rate constants of DMABN and furfuryl alcohol (FFA) relevant to the characterization of the impact of singlet oxygen on the photosensitized transformation of DMABN.

Solution components [a]	$k_{DMABN}^{obs,c}$ **(10^{-4} s^{-1})** [b]		$k_{FFA}^{obs,c}$ **(10^{-4} s^{-1})** [b]		**$[^1O_2]_{ss}$ (10^{-12} M)** [c]	
	H_2O	**D_2O**	**H_2O**	**D_2O**	**H_2O**	**D_2O**
none [d]	0.14±0.03	n.d. [e]	<0.05	n.d.	<0.04	n.d.
NaN_3 [d, f]	0.99±0.08	n.d.	n.d.	n.d.	n.d.	n.d.
PLFA [d]	5.9±0.6	6.3±0.6	1.9±0.2	18.8±1.2	1.6±0.2	22.7±1.5
PLFA, NaN_3 [d]	4.5±0.7	5.1±0.9	1.1±0.4	1.1±0.4	0.9±0.4	1.4±0.5
Rose Bengal (RB) [g, h]	1.80±0.11	1.92±0.17	11.6±0.4	125±30	9.7±0.3	150±36
RB, NaN_3 [g, h]	2.08±0.18	1.30±0.17	0.95±0.19	0.96±0.2	0.79±0.16	1.2±0.3

Notes:

[a] In addition to DMABN ($[DMABN]_0$=5.0 μM), FFA ($[FFA]_0$=5.0 μM) and phosphate (5.0 mM, pH 8.0). Initial concentrations of further components: $[PLFA]_0$=5.0 mg_C L^{-1}; $[RB]_0$=2.0 μM; $[NaN_3]_0$=10.0 mM.

[b] No correction performed for the constants given in the first two rows.

[c] Steady-state concentration of singlet oxygen determined as $k_{FFA}^{obs,c} / k_{FFA,^1O_2}^{r}$ (see text for details).

[d] Irradiation setup with 500 W MP Hg lamp and filter solution for λ>320 nm.

[e] n.d.: not determined.

[f] Solution did not contain FFA.

[g] Irradiation setup with 150 W MP Hg lamp, filter solution for λ>380 nm and steel wire cloth filter.

[h] All rate constants corrected for the photodegradation RB during irradiation (see SI, Text S7).

Photosensitization and inhibition by fulvic acids, and DOM concentration dependence. Figure 2 shows the dependence of the phototransformation rate constant of DMABN on DOM concentration. Direct phototransformation was drastically reduced with respect to the solar simulator setup, and photosensitization by DOM was dominant for [DOM]>≈0.2 mg_C L^{-1}. Overall a steady, non-linear increase in rate constant with increasing DOM concentration for both fulvic acids is apparent, while at low DOM concentration (<1.0 mg_C L^{-1}) a linear relationship is observed (see inset in Figure 2). The dependence of the rate constants on DOM concentration is similar to that of sulfadiazine in PLFA solutions[20] and of tryptophan in solutions of various humic substances.[21] This behavior was interpreted in terms of the antagonistic photosensitizing and inhibitory effects of DOM on $^3DOM^*$-induced transformation of the target compounds.

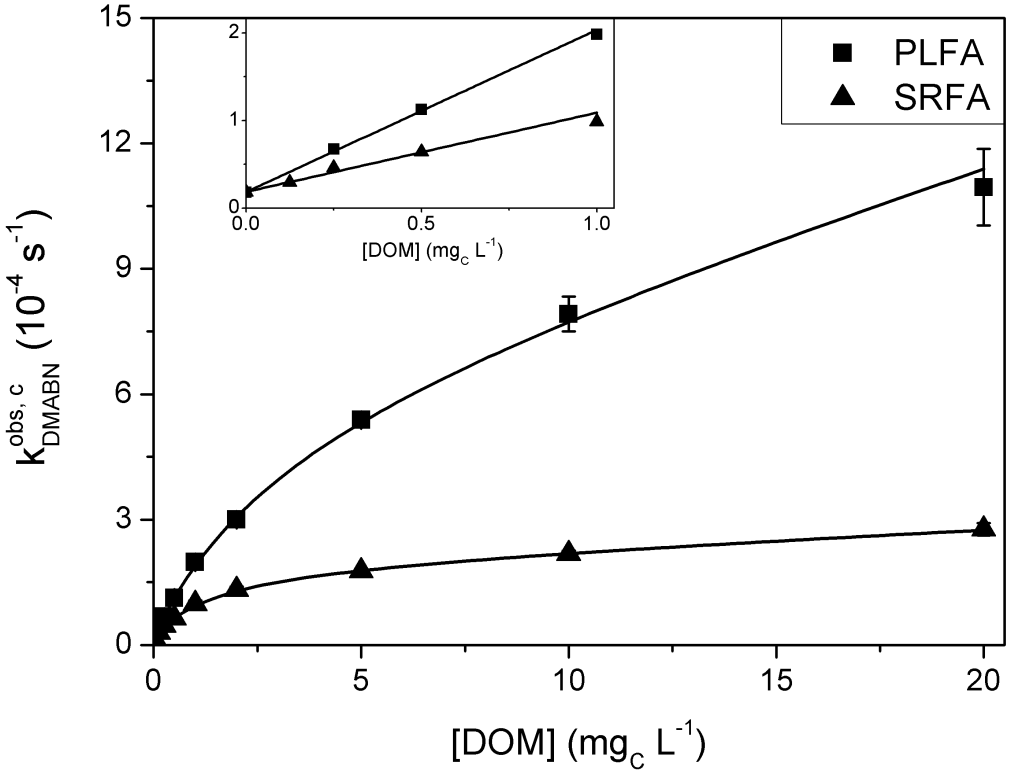

Figure 2. Effect of DOM concentration (Pony Lake fulvic acid (PLFA, black squares); Suwannee River fulvic acid (SRFA, black triangles)) on the corrected pseudo-first-order phototransformation rate constant of DMABN (5 μM initial concentration). Results obtained from merry-go-round photoreactor experiments (λ>320 nm). Lines are non-linear fits to equation 2. Error bars represent 95% confidence intervals obtained from linear regression. Inset: enlarged view for low DOM concentrations (≤1.0 $mg_C\ L^{-1}$) with linear regression lines.

To analyze the rate constant data from Figure 2, a two-channel reaction model for inhibition of triplet-induced oxidation[17] was extended to include photosensitization by DOM. The derivation of the kinetic equations for such an extended model is given in detail the SI, Text S8. The resulting pseudo-first-order rate constant for the photosensitized transformation, k_{TC}^{sens}, is described by equation 2, where the first term on the right-hand side, β[DOM], accounts for a photosensitization directly proportional to the DOM concentration, and the fractional term accounts for inhibition.

$$k_{TC}^{sens}(\mathrm{DOM}) = \beta[\mathrm{DOM}]\frac{1+[\mathrm{DOM}]/[\mathrm{DOM}]_{1/2}(1-f)}{1+[\mathrm{DOM}]/[\mathrm{DOM}]_{1/2}} \qquad (2)$$

In equation 2, β is a proportionality factor that accounts for photoinduced formation of $^3DOM^*$, deactivation of $^3DOM^*$ and its reaction with the target compound, f is the fraction of photosensitized reaction intermediates susceptible to inhibition by DOM,[17] and $[DOM]_{1/2}$ is the concentration of DOM required to achieve half of the maximum rate constant reduction obtainable by inhibition. According to equation 2, two limiting cases for k_{TC}^{sens} are possible: (a)

At low DOM concentration ([DOM]<<$[DOM]_{1/2}$), the fraction in equation 2 becomes unity and the rate constant reduces the mere photosensitization term, as given by equation 3. (b) At high DOM concentration ([DOM]>>$[DOM]_{1/2}$), equation 4 is obtained.

$$k_{TC}^{sens} = \beta[\mathrm{DOM}] \quad (3)$$

$$k_{TC}^{sens} = \beta[\mathrm{DOM}]_{1/2} + \beta[\mathrm{DOM}](1-f) \quad (4)$$

Interestingly, for 100% formation of intermediates susceptible to inhibition (i.e., f=1) equation 4 reduces to the constant term $\beta[DOM]_{1/2}$, whereas in all other cases an asymptotic linear increase with increasing DOM concentrations is predicted with $\beta(1-f)$ as slope.

To fit the data in Figure 2, the corrected phototransformation rate constant was assumed to consist of the contributions from direct (k_{TC}^{dir}) and indirect (k_{TC}^{sens}) phototransformation, as given by equation 5.

$$k_{TC}^{obs,c} = k_{TC}^{dir} + k_{TC}^{sens} \quad (5)$$

Equations 2 and 3, with the addition of a constant offset accounting for k_{TC}^{dir}, were used to fit the whole rate constant data and the data for [DOM]≤1.0 $mg_C\ L^{-1}$, respectively. The assumption of a constant k_{TC}^{dir} is not strictly valid, because k_{TC}^{dir} is probably also affected by DOM inhibition (see the effect of phenol shown in Figure 1), but is an acceptable approximation considering the very small value of k_{TC}^{dir}. As demonstrated by the trend lines in Figure 2 and the numerical results collected in Table 2, both equations provided good fits.

Table 2. Parameters for the photosensitizing and inhibitory effects of PLFA and SRFA on the phototransformation of DMABN obtained from data fitting. [a]

Data series	β_1 [b] (10^{-4} L mg_C^{-1} s^{-1})	$[DOM_1]_{1/2}$ [c] (mg_C L^{-1})	β_2 [b] (10^{-4} L mg_C^{-1} s^{-1})	$[DOM_2]_{1/2}$ [c] (mg_C L^{-1})	$[PhOH]_{1/2}$ (μM)	f [d]	Adjusted R^2
	(DOM_1=PLFA)		(DOM_2=SRFA)				
PLFA only data (Figure 2)	2.14 ±0.19	3.2±1.2	n.a. [e]	n.a.	n.a.	0.86±0.06	0.999
SRFA only data (Figure 2)	n.a.	n.a.	1.21 ±0.15	1.5±0.4	n.a.	0.963 ±0.015	0.998
PLFA (5 mg_C L^{-1}) and SRFA data (Figure 3)	*2.14 (fixed)*	4.8±0.2	*1.21 (fixed)*	1.48±0.15	n.a.	0.967 ±0.008	0.994
PLFA (5 mg_C L^{-1}) and PhOH data (Figure 4)	*2.14 (fixed)*	3.3±1.0	n.a.	n.a.	3.7±1.2	*0.85 (fixed)*	0.961
PLFA (5 mg_C L^{-1}) and PhOD [e] data (Figure 4)	*2.14 (fixed)*	3.4±0.3	n.a.	n.a.	4.4±0.6	*0.85 (fixed)*	0.989
PLFA (5 mg_C L^{-1}) and SRFA difference data (Figure 4)	*2.14 (fixed)*	4.5±0.3	n.a.	1.5±0.3	n.a.	0.93±0.02	0.998

390 Notes:
391 [a] Errors indicate 95% confidence intervals obtained from the non-linear regressions using equation 2 (data from Figure 2), equation 6
392 (data from Figure 3), or equation 7 (data from Figure 4).
393 [b] Proportionality factor accounting for the photosensitizing effect of DOM (see equation 2): β_1 for PLFA and β_2 for SRFA.
394 [c] Concentration of DOM (PLFA or SRFA) required to achieve half of the maximum rate constant reduction obtainable by inhibition
395 (see equation 2).
396 [d] Fraction of photosensitized reaction intermediates susceptible to inhibition by DOM (see equation 2).
397 [e] n.a.: not applicable.
398 [f] Mono deuterated PhOH, resulting from proton exchange in the solvent D_2O.
399

Photosensitization and inhibition in solutions with mixed DOMs and in natural water mixtures. In surface freshwaters the composition of DOM is often the result of mixing of waters containing DOM from differing sources. To show exemplarily how such mixing processes may affect the inhibitory properties of DOM, irradiation experiments were performed utilizing a fixed concentration of primarily photosensitizing and weakly inhibitory DOM, and variable concentrations of weakly photosensitizing and strongly inhibitory DOM. PLFA and the DOM in GW were employed as the mainly photosensitizing (and poorly inhibitory) DOMs, according to the results of previous studies.[17-19] To be noted is the mainly autochtonous origin of these materials, which correlates with their relatively low specific absorption coefficient ($SUVA_{254}$, measured at the wavelength of 254 nm, see SI, Tables S1 and S2). SRFA and the DOM in EG were selected as strongly inhibitory DOM due to their primarily allochtonous origin. Both exhibit higher specific absorption coefficient than PLFA and the DOM in GW, indicating higher aromaticity.

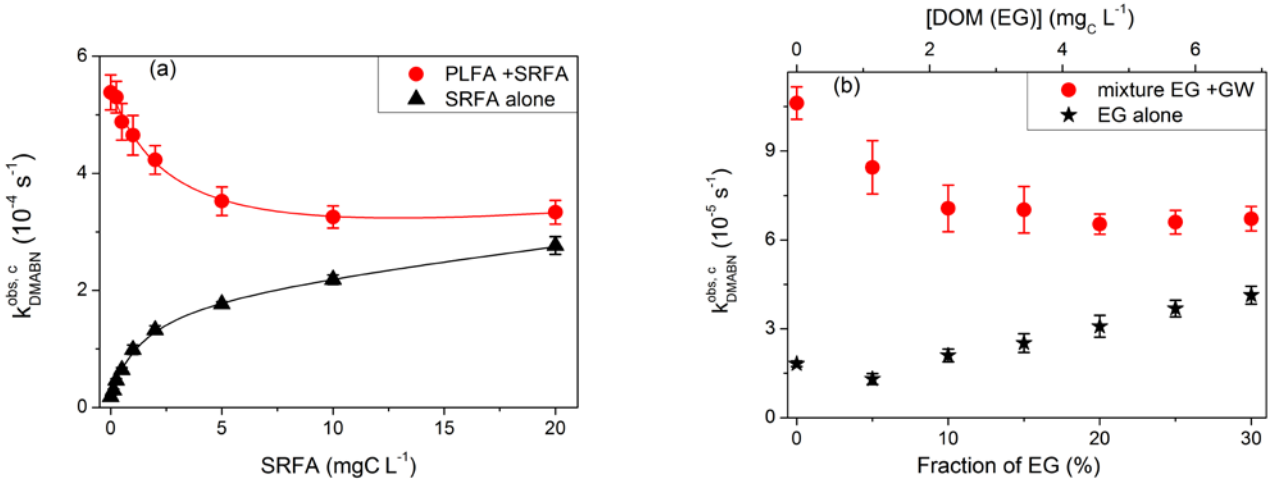

Figure 3. Pseudo-first-order phototransformation rate constants of DMABN in (a) solutions containing 0 mg_C L^{-1} (black triangles, same data as in Figure 2) or 5 mg_C L^{-1} (red circles) of Pony Lake fulvic acid (PLFA) and varying concentrations of Suwannee River fulvic acid (SRFA), and (b) solutions containing a constant volumetric fraction of GW (0% (black stars) or 68.5% (red

circles), the latter corresponding to 2.26 $mg_C\ L^{-1}$), varying volumetric fractions of EG and ultrapure water (the remaining volumetric fraction to give 100%). Results obtained from merry-go-round photoreactor experiments (λ>320 nm). Lines are non-linear fits to equation 2 (black) and equation 6 (red). Error bars represent 95% confidence intervals from linear regressions (equation 1).

Figure 3 shows that an increase in concentration of strongly inhibiting DOM leads to a decrease in the rate constant for the phototransformation of DMABN. The complete rate constant equation describing photosensitizing and inhibitory effects in a mixture of two different DOMs (derived in analogy to equation 2, see SI, Text S9) can be formulated as:

$$k_{TC}^{sens}(\mathrm{DOM}_1, \mathrm{DOM}_2) = \left(\beta_1[\mathrm{DOM}_1] + \beta_2[\mathrm{DOM}_2]\right)\frac{1 + \left\{[\mathrm{DOM}_1]/[\mathrm{DOM}_1]_{1/2} + [\mathrm{DOM}_2]/[\mathrm{DOM}_2]_{1/2}\right\}(1-f)}{1 + [\mathrm{DOM}_1]/[\mathrm{DOM}_1]_{1/2} + [\mathrm{DOM}_2]/[\mathrm{DOM}_2]_{1/2}} \qquad (6)$$

Analogous equations can be derived for a higher number of differing DOMs (see SI, Text S9, equation S20). Rate constant data for solutions containing PLFA (≡DOM_1) and SRFA (≡DOM_2) (Figure 3a, red circles) were fit to equation 6 with the fixed parameters [PLFA]=5 $mg_C\ L^{-1}$, β_1 and β_2 (from the fittings to equation 2, see Table 2), the three fitting parameters $[PLFA]_{1/2}$, $[SRFA]_{1/2}$ and *f*, and [SRFA] as the independent variable. The fit was excellent and the obtained values of the fitting parameters (See Table 2) were in good agreement with those obtained from single DOM series (Figure 2). Attempts to extract reasonably accurate fitting parameters from the data of the natural water mixtures failed, probably due to the restricted range of studied DOM concentrations and the low rate constants. However, qualitative trends are similar as observed for the PLFA/SRFA mixtures. Note that in the absence of a mutual inhibitory effect, the

phototransformation rate constants would be additive, and a steady increase would be expected. Such a scenario (with no inhibition) was tested for mixtures of GW and EG by using furfuryl alcohol (FFA) as a target compound. FFA is known to undergo photosensitized oxygenation by singlet molecular oxygen, and its phototransformation should only reflect the photosensitizing properties of DOM, while inhibitory effects should be absent. The observed linear and identical increases (with the same slope) of the phototransformation rate constant of FFA in the presence and absence of GW fully confirmed the expectations (see SI, Figure S7).

Inhibitory effect of phenol as a model antioxidant. Phenolic compounds have been shown to cause inhibition of triplet-induced oxidations analogously to DOM and have therefore been used as model inhibitors.[18, 20] To further characterize the inhibitory process in the indirect phototransformation of DMABN, phenol was employed at variable concentrations to inhibit transformation of DMABN photosensitized by 5.0 mg_C L^{-1} of PLFA (see Figure 4).

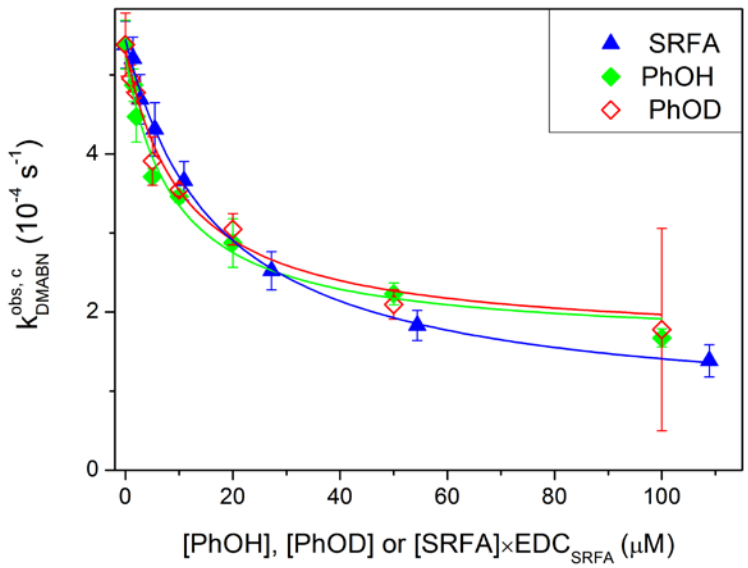

Figure 4. Corrected and normalized pseudo-first-order rate constants for the transformation of DMABN photosensitized by Pony Lake fulvic acid (PLFA, 5.0 mg_C L^{-1}) and their dependence on

464 the concentration of added phenol (PhOH, green diamonds) and mono-deuterated phenol (PhOD,
465 open red diamonds). PhOD experiments were performed in D_2O solutions (D atom fraction of
466 ~94%). Results obtained from merry-go-round photoreactor experiments (λ>320 nm). The rate
467 constants were corrected for quenching of $^3PLFA^*$ by phenol (see SI, Text S6). For comparison,
468 the net inhibitory effect of Suwannee River fulvic acid (SRFA) in terms of concentration of
469 available electrons (see text for calculations) is also shown. Lines are non-linear fits to equation
470 7 (phenol data) or equation 6 modified by subtracting term 8 (SRFA data, see text). Error bars
471 represents 95% confidence interval from linear regressions (equation 1).

472 The rate constants for DMABN phototransformation decreased nonlinearly with increasing
473 phenol concentration, approaching a reduction of about 60% at 100 μM phenol. Note that the
474 rate constants displayed in Figure 4 were corrected for quenching of $^3PLFA^*$ by phenol, which
475 was measured using furfuryl alcohol as a probe compound and the methods described in the SI,
476 Text S6. The effect of adding deuterated phenol (experiments performed in D_2O) was the same
477 as for phenol. This constitutes an important piece of evidence that the reduction of the oxidation
478 intermediate of DMABN, probably the $DMABN^{\cdot+}$ radical cation, does not involve a hydrogen
479 atom abstraction from the phenolic functional group in the rate-determining reaction step. The
480 data of the phenol series (with phenol (PhOH) or its mono-deuterated form (PhOD)) from Figure
481 4 fitted well to equation 7, which was derived from equation 6 by setting PLFA≡DOM_1 and
482 substituting DOM_2 with PhOH (or PhOD). Since phenol has no photosensitizing effect, β_2=0.

483 $$k_{TC}^{sens}(\mathrm{PLFA},\mathrm{PhOH}) = \beta_1[\mathrm{PFLA}]\frac{1+\{[\mathrm{PLFA}]/[\mathrm{PLFA}]_{1/2}+[\mathrm{PhOH}]/[\mathrm{PhOH}]_{1/2}\}(1-f)}{1+[\mathrm{PLFA}]/[\mathrm{PLFA}]_{1/2}+[\mathrm{PhOH}]/[\mathrm{PhOH}]_{1/2}} \quad (7)$$

Among the obtained fitting parameters, collected in Table 2, $[PLFA]_{1/2}$ values were very similar to the fitting of PLFA only data (Figure 2, equation 2). To compare quantitatively the inhibitory effect of phenol and antioxidant moieties in SRFA, the concentration of the latter antioxidant moieties was calculated by multiplying the electron donating capacity (EDC) of SRFA with its concentration. The published EDC value for pH 7 and an oxidizing potential of E_h=+0.73 V,[38] i.e., 2.848 $mmol_{e^-}\ g_{SRFA}^{-1}$ (corresponding to 5.47 $\mu mol_{e^-}\ mg_C^{-1}$, considering the carbon content of SRFA given in the same reference) was used for this purpose. The obtained average $[SRFA]_{1/2}$×EDC value (≈8.2 $\mu mol_{e^-}\ L^{-1}$) is about twice as large as $[PhOH]_{1/2}$, indicating an overall lower reactivity of the phenolic moieties of SRFA compared to phenol. Figure 4 also shows, for comparison with the phenol data, the rate constants from Figure 3 corrected by subtracting the following term, which quantifies the contribution of SRFA to the photosensitized transformation of DMABN:

$$\beta_2[\mathrm{DOM}_2]\frac{1+\{[\mathrm{DOM}_1]/[\mathrm{DOM}_1]_{1/2}+[\mathrm{DOM}_2]/[\mathrm{DOM}_2]_{1/2}\}(1-f)}{1+[\mathrm{DOM}_1]/[\mathrm{DOM}_1]_{1/2}+[\mathrm{DOM}_2]/[\mathrm{DOM}_2]_{1/2}} \quad (8)$$

These corrected rate constants, represented by the blue triangles in Figure 4, show a similar trend as the lines describing the inhibitory effect of phenol. At low concentrations, the inhibitory effect of SRFA appears to be less important than for PhOH/PhOD, which is reflected in the higher $[SRFA]_{1/2}$×EDC value than $[PhOH]_{1/2}$ as discussed above. At higher concentrations, SRFA seems to be at least as an efficient inhibitor as phenol, which may be related to the higher value of *f* obtained for the fittings regarding SRFA. An accurate quantitative comparison appears to be difficult due to the uncertainty of the various parameters used in the model. Overall, one can affirm that $[SRFA]_{1/2}$×EDC is of the same order of magnitude as $[PhOH]_{1/2}$. This confirms the conclusions of a similar comparison performed using sulfonamide data[18] and concurs with the

antioxidant hypothesis as the cause of inhibition for the photosensitized transformation of DMABN.

Characterization of product formation. The main peak appearing in the HPLC chromatograms (see SI, Figure S8) during the phototransformation of DMABN was identified as its mono-demethylated derivative, 4-methylaminobenzonitrile (MABN), by comparison of its HPLC retention time and UV absorption spectra with those of commercially available MABN. The kinetics of DMABN depletion and MABN formation during irradiation in the presence of PLFA or RB as photosensitizers are shown in Figure 5. The efficiency of formation of MABN from DMABN transformation (moles of MABN formed per mole of DMABN consumed), expressed as the selectivity factor γ, can be estimated by assuming the following system of reactions (see also SI, Scheme S3), which considers the transformation of DMABN to either MABN (equation 9) or other products (equation 10) in a first step, and transformation of MABN to further products (equation 11).

$$\mathrm{DMABN} \xrightarrow{k_1 \times \gamma} \mathrm{MABN} \tag{9}$$

$$\mathrm{DMABN} \xrightarrow{k_1 \times (1-\gamma)} \mathrm{products}_1 \tag{10}$$

$$\mathrm{MABN} \xrightarrow{k_2} \mathrm{products}_2 \tag{11}$$

As shown in the SI, Text S13, the kinetics of MABN in a solution initially containing DMABN as the only target compound can be described by the following equation:

$$[\mathrm{MABN}] = [\mathrm{DMABN}]_0 \gamma \frac{k_1}{k_2 - k_1} \left(e^{-k_1 t} - e^{-k_2 t} \right) \tag{12}$$

The pseudo-first-order rate constants k_1 and k_2 for the phototransformation of DMABN and MABN, respectively, were determined in two separate experiments initially containing 5.0 μM of DMABN (see data in Figure 5) or MABN (see SI, Figure S9). The selectivity factor γ was obtained by fitting the [MABN] data (Figure 5) to equation 12 (γ was the only fitting parameter). For the kinetic experiments illustrated in Figure 5, γ values of 72±4% and 81±2% were obtained for the PLFA and RB systems, respectively.

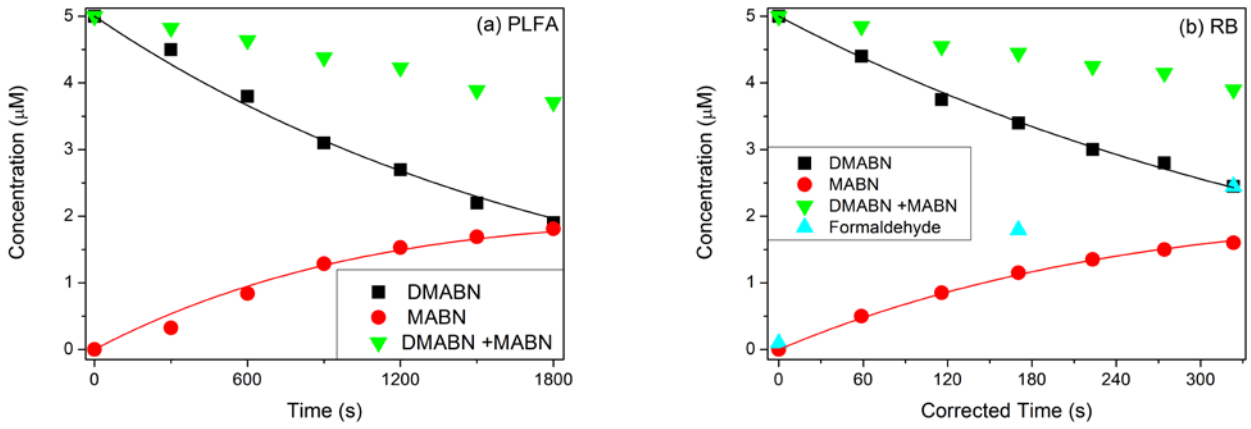

Figure 5. Phototransformation kinetics of DMABN (5.0 μM initial concentration) and concomitant *N*-methyl-4-cyanoaniline (MABN) formation in the presence of (a) 5mg$_C$ L^{-1} PLFA and (b) 5 μM RB (time axis scale corrected to account for RB photobleaching, see SI, Text S7). Results obtained from merry-go-round photoreactor experiments with (a) λ>320 nm, and (b) λ>370 nm. Green triangles represent the sum of DMABN and MABN. Black lines represent non-linear fits to a first-order rate law. Red lines represent non-linear fits to equation 12. In (b) blue triangles represent formaldehyde concentration.

The loss of the methyl group upon photosensitized transformation can be rationalized in terms of the reaction mechanisms presented in Scheme 1. Derivatives of the *N*,*N*-dimethylaniline radical

cation, such as DMABN$^{\cdot+}$, are known to tautomerize to yield a carbon-centered radical,[39] which can then deprotonate and react with oxygen to form a peroxyl radical.[40] The latter releases superoxide and the so formed imine is hydrolyzed yielding the demethylated aniline and formaldehyde. The formation of formaldehyde was confirmed in the present irradiation experiments using RB as a photosensitizer (Figure 5b). Though the mechanism predicts 1:1 formation of MABN and formaldehyde, the concentration of the latter after 30% and 50% transformation of DMABN was higher than the concentration of MABN. This is probably due to the transformation of MABN yielding 4-cyanoaniline and formaldehyde.

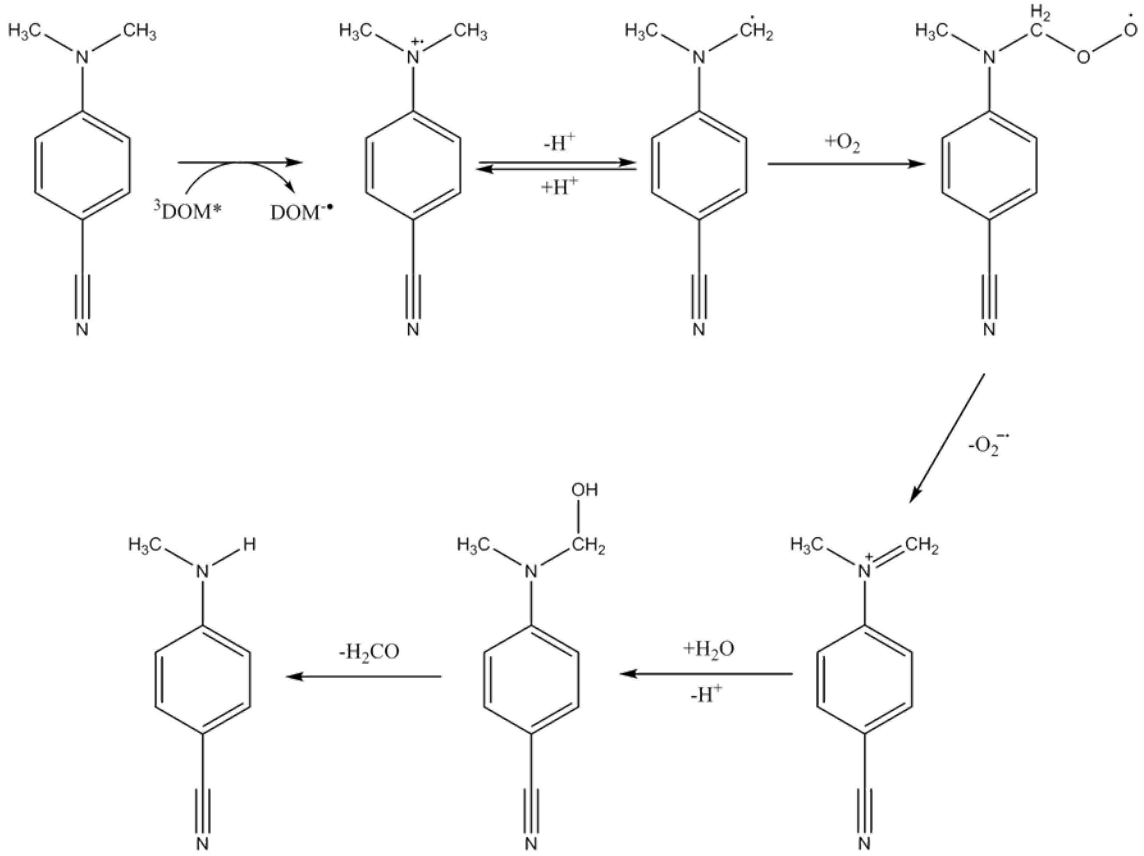

Scheme 1. Proposed main reaction pathway for the transformation of DMABN photosensitized by DOM.

Because γ values are lower than unity (by 10–30%), a fraction of DMABN is expected to react through another, still unknown reaction pathway compared to Scheme 1. It has to be noted that γ has a different meaning from *f*, which is the fraction of DMABN molecules that can be inhibited in their transformation by the presence of antioxidants. The fact that γ and *f* values are similar does not imply that the non-inhibiting reaction channel corresponds to the process yielding reaction products other than MABN. Supplementary experiments performed with PLFA as the photosensitizer (conditions as for the data in Figure 5) with the addition of phenol as an antioxidant revealed that the selectivity factor γ remained constant in the phenol concentration range of 0–50 μM (see SI, Table S7). This result concurs with the assumption that antioxidants are exclusively involved in the reduction of $DMABN^{\cdot+}$ to the parent compound and do not affect the subsequent reactions.

ENVIRONMENTAL IMPLICATIONS

The previously developed two-channel model accounting for partial inhibition of triplet-induced oxidation[17] was employed successfully in this study to describe the photosensitized transformation kinetics of DMABN in aqueous solutions containing binary mixtures of DOM. Equation 6 could be useful in the prediction of rate constants for the photosensitized transformation of aromatic amine contaminants in surface waters that are affected by organic matter input from various origins. Taking the binary mixture of PLFA and SRFA as characterized in this study as an example, one can construct surface plots as shown in Figure 6a. In addition to the features already discussed for two-dimensional plots (Figures 2 and 3), Figure 6a also comprises contour lines, which indicate that a given value of the rate constant

corresponds to a set of different concentrations of both DOMs. It can be seen that, moving on a contour line from left to right, the concentration of PLFA is only slightly reduced, while there is a big change in SRFA concentration. A situation corresponding to such a scenario was possibly observed for the phototransformation rate constant of sulfadiazine in water samples taken along the course of a river.[20] In that study, only a little increase in the sulfadiazine phototransformation rate constant was observed in going from a low DOC pristine water near the source of the river to an increasingly wastewater-impacted river water with higher DOC. An alternative graphical representation of the same function displayed in Figure 6a is shown in Figure 6b, in which the fraction X_1=[DOM_1]/([DOM_1]+[DOM_2]) of a the first DOM in the mixture ($0 \leq X_1 \leq 1$) and the total DOM concentration DOC=[DOM_1]+[DOM_2] were chosen as the independent variables (see SI, Text S14). For a given constant fraction X_1, dependencies of k_{TC}^{sens} vs. DOC have a similar curved shape as and are between the two lines shown in Figure 2. Moreover, for a constant DOC and varying X_1, convex lines connecting the two extremes in reactivity are observed. We envisage the application of the present concept and graphs to estimate the variability in photoreactivity of compounds such as DMABN (i.e., those affected by DOM-induced photosensitization and inhibition) in surface waters strongly impacted by wastewater effluents from varying degrees of wastewater treatment. However, we would like to point out that the considerations made in this section are restricted to DOM-photosensitized transformations following the sensitization and inhibition models applied in this study. In case of important direct phototransformation or other photosensitized reaction channels, as recently addressed by McNeill and coworkers,[21] a more comprehensive approach has to be adopted.

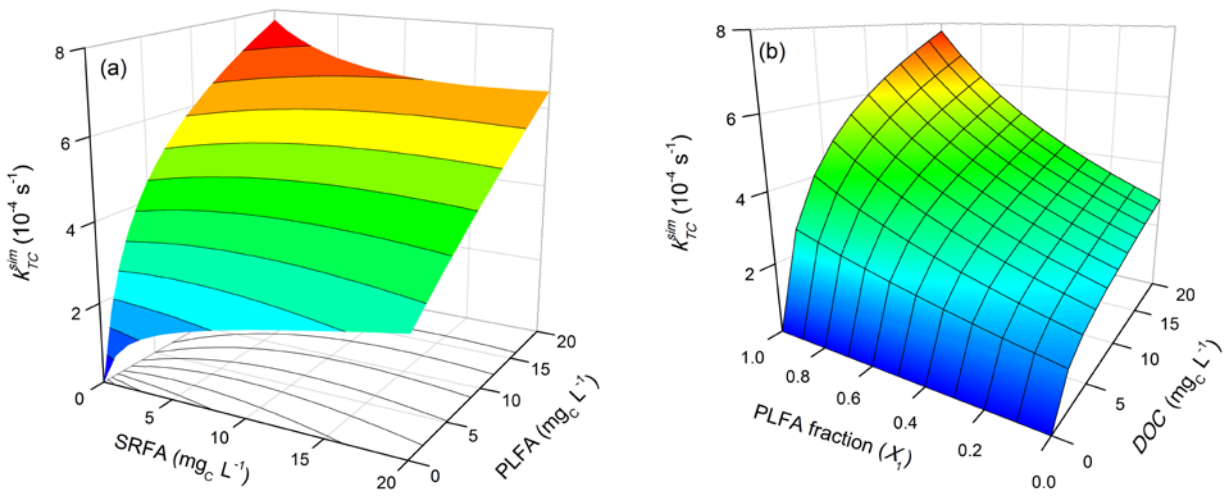

Figure 6. Surface plots representing the DOM-concentration dependence of the rate constant (k_{TC}^{sim}) for the transformation of a target contaminant photosensitized and inhibited by a binary mixture of DOM (PLFA and SRFA). Parameter values for PLFA and SRFA determined in this study for DMABN (see Table 2, third line) were applied. (a) Representation of equation 6, where contour lines (for fixed k_{TC}^{sim} values) are given on the surface plot and shown as projections on the x-y plane; (b) Representation of equation S34 (see text and SI, Text S14).

ASSOCIATED CONTENT

Supporting Information.

The Supporting Information is available free of charge on the ACS Publications website at DOI:.

Additional figures, tables, experimental details and derivation of equations.

AUTHOR INFORMATION

Corresponding Author

* E-mail: silvio.canonica@eawag.ch. Telephone: +41-58-765-5453. Fax: +41-58-765-5028.

Funding Sources

This work was supported by the Swiss National Science Foundation (Project No. 200021-140815).

Notes

The authors declare no competing financial interests.

ACKNOWLEDGMENTS

The authors would like to thank Elisabeth Salhi and Ursula Schönenberger for laboratory support and Fernando Rosario-Ortiz for helpful discussions and reviewing the manuscript.

636 REFERENCES

637 1. Canonica, S.; Jans, U.; Stemmler, K.; Hoigné, J. Transformation kinetics of phenols in
638 water: Photosensitization by dissolved natural organic material and aromatic ketones. *Environ.*
639 *Sci. Technol.* **1995,** *29* (7), 1822-1831.

640 2. Chin, Y. P.; Miller, P. L.; Zeng, L. K.; Cawley, K.; Weavers, L. K. Photosensitized
641 degradation of bisphenol A by dissolved organic matter. *Environ. Sci. Technol.* **2004,** *38* (22),
642 5888-5894.

643 3. Felcyn, J. R.; Davis, J. C. C.; Tran, L. H.; Berude, J. C.; Latch, D. E. Aquatic
644 photochemistry of isoflavone phytoestrogens: Degradation kinetics and pathways. *Environ. Sci.*
645 *Technol.* **2012,** *46* (12), 6698-6704.

646 4. Kelly, M. M.; Arnold, W. A. Direct and indirect photolysis of the phytoestrogens
647 genistein and daidzein. *Environ. Sci. Technol.* **2012,** *46* (10), 5396-5403.

648 5. Canonica, S.; Freiburghaus, M. Electron-rich phenols for probing the photochemical
649 reactivity of freshwaters. *Environ. Sci. Technol.* **2001,** *35* (4), 690-695.

650 6. Canonica, S.; Laubscher, H. U. Inhibitory effect of dissolved organic matter on triplet-
651 induced oxidation of aquatic contaminants. *Photochem. Photobiol. Sci.* **2008,** *7* (5), 547-551.

652 7. Boreen, A. L.; Arnold, W. A.; McNeill, K. Triplet-sensitized photodegradation of sulfa
653 drugs containing six-membered heterocyclic groups: Identification of an SO_2 extrusion
654 photoproduct. *Environ. Sci. Technol.* **2005,** *39* (10), 3630-3638.

655 8. Guerard, J. J.; Chin, Y. P.; Mash, H.; Hadad, C. M. Photochemical fate of
656 sulfadimethoxine in aquaculture waters. *Environ. Sci. Technol.* **2009,** *43* (22), 8587-8592.

657 9. Luo, X. Z.; Zheng, Z.; Greaves, J.; Cooper, W. J.; Song, W. H. Trimethoprim: Kinetic
658 and mechanistic considerations in photochemical environmental fate and AOP treatment. *Water*
659 *Res.* **2012,** *46* (4), 1327-1336.

660 10. Guerard, J. J.; Chin, Y. P. Photodegradation of ormetoprim in aquaculture and stream-
661 derived dissolved organic matter. *J. Agric. Food Chem.* **2012,** *60* (39), 9801-9806.

662 11. Gerecke, A. C.; Canonica, S.; Müller, S. R.; Schärer, M.; Schwarzenbach, R. P.
663 Quantification of dissolved natural organic matter (DOM) mediated phototransformation of
664 phenylurea herbicides in lakes. *Environ. Sci. Technol.* **2001,** *35* (19), 3915-3923.

665 12. Zeng, T.; Arnold, W. A. Pesticide photolysis in prairie potholes: Probing photosensitized
666 processes. *Environ. Sci. Technol.* **2013,** *47* (13), 6735-6745.

667 13. Canonica, S.; Hellrung, B.; Wirz, J. Oxidation of phenols by triplet aromatic ketones in
668 aqueous solution. *J. Phys. Chem. A* **2000,** *104* (6), 1226-1232.

669 14. Canonica, S.; Hellrung, B.; Müller, P.; Wirz, J. Aqueous oxidation of phenylurea
670 herbicides by triplet aromatic ketones. *Environ. Sci. Technol.* **2006,** *40* (21), 6636-6641.

671 15. Erickson, P. R.; Walpen, N.; Guerard, J. J.; Eustis, S. N.; Arey, J. S.; McNeill, K.
672 Controlling factors in the rates of oxidation of anilines and phenols by triplet methylene blue in
673 aqueous solution. *J. Phys. Chem. A* **2015,** *119* (13), 3233-3243.

16. Jonsson, M.; Lind, J.; Eriksen, T. E.; Merényi, G. Redox and acidity properties of 4-substituted aniline radical cations in water. *J. Am. Chem. Soc.* **1994,** *116* (4), 1423-1427.

17. Wenk, J.; von Gunten, U.; Canonica, S. Effect of dissolved organic matter on the transformation of contaminants induced by excited triplet states and the hydroxyl radical. *Environ. Sci. Technol.* **2011,** *45* (4), 1334-1340.

18. Wenk, J.; Canonica, S. Phenolic antioxidants inhibit the triplet-induced transformation of anilines and sulfonamide antibiotics in aqueous solution. *Environ. Sci. Technol.* **2012,** *46* (10), 5455-5462.

19. Wenk, J.; Aeschbacher, M.; Sander, M.; von Gunten, U.; Canonica, S. Photosensitizing and inhibitory effects of ozonated dissolved organic matter on triplet-induced contaminant transformation. *Environ. Sci. Technol.* **2015,** *49* (14), 8541-8549.

20. Bahnmüller, S.; von Gunten, U.; Canonica, S. Sunlight-induced transformation of sulfadiazine and sulfamethoxazole in surface waters and wastewater effluents. *Water Res.* **2014,** *57*, 183-192.

21. Janssen, E. M. L.; Erickson, P. R.; McNeill, K. Dual roles of dissolved organic matter as sensitizer and quencher in the photooxidation of tryptophan. *Environ. Sci. Technol.* **2014,** *48* (9), 4916-4924.

22. Ulrich, M. M.; Muller, S. R.; Singer, H. P.; Imboden, D. M.; Schwarzenbach, R. P. Input and dynamic behavior of the organic pollutants tetrachloroethene, atrazine, and NTA in a lake: A study combining mathematical modeling and field measurements. *Environ. Sci. Technol.* **1994,** *28* (9), 1674-1685.

23. Wegelin, M.; Canonica, S.; Mechsner, K.; Fleischmann, T.; Pesaro, F.; Metzler, A. Solar water disinfection: Scope of the process and analysis of radiation experiments. *J. Water Supply Res. Technol. - Aqua* **1994,** *43* (3), 154-169.

24. Huntscha, S.; Singer, H.; Canonica, S.; Schwarzenbach, R. P.; Fenner, K. Input dynamics and fate in surface water of the herbicide metolachlor and of its highly mobile transformation product metolachlor ESA. *Environ. Sci. Technol.* **2008,** *42* (15), 5507-5513.

25. Dulin, D.; Mill, T. Development and evaluation of sunlight actinometers. *Environ. Sci. Technol.* **1982,** *16* (11), 815-820.

26. Nash, T. The colorimetric estimation of formaldehyde by means of the Hantzsch reaction. *Biochem. J.* **1953,** *55* (3), 416-421.

27. Flyunt, R.; Leitzke, A.; Mark, G.; Mvula, E.; Reisz, E.; Schick, R.; von Sonntag, C. Determination of $^{\bullet}OH$, $O_2^{\bullet-}$, and hydroperoxide yields in ozone reactions in aqueous solution. *J. Phys. Chem. B* **2003,** *107* (30), 7242-7253.

28. Andreozzi, R.; Marotta, R.; Paxeus, N. Pharmaceuticals in STP effluents and their solar photodegradation in aquatic environment. *Chemosphere* **2003,** *50* (10), 1319-1330.

29. Liu, Q. T.; Williams, H. E. Kinetics and degradation products for direct photolysis of beta-blockers in water. *Environ. Sci. Technol.* **2007,** *41* (3), 803-810.

30. Jasper, J. T.; Sedlak, D. L. Phototransformation of wastewater-derived trace organic contaminants in open-water unit process treatment wetlands. *Environ. Sci. Technol.* **2013,** *47* (19), 10781-10790.

31. Alder, A. C.; Schaffner, C.; Majewsky, M.; Klasmeier, J.; Fenner, K. Fate of beta-blocker human pharmaceuticals in surface water: Comparison of measured and simulated concentrations in the Glatt Valley Watershed, Switzerland. *Water Res.* **2010,** *44* (3), 936-948.

32. Loeff, I.; Rabani, J.; Treinin, A.; Linschitz, H. Charge-transfer and reactivity of nπ* and ππ* organic triplets, including anthraquinonesulfonates, in interactions with inorganic anions: A comparative study based on classical Marcus theory. *J. Am. Chem. Soc.* **1993,** *115* (20), 8933-8942.

33. Köhler, G.; Getoff, N.; Rotkiewicz, K.; Grabowski, Z. R. Electron photoejection from donor–aryl-acceptor molecules in aqueous solution. *J. Photochem.* **1985,** *28* (4), 537-546.

34. Larson, R. A.; Marley, K. A. Singlet oxygen in the environment. In *The Handbook of Environmental Chemistry*, Hutzinger, O., Ed. Springer: Berlin, Germany, 1999; Vol. 2, Part L, pp 123-137.

35. Rodgers, M. A. J.; Snowden, P. T. Lifetime of O_2 ($^1\Delta_g$) in liquid water as determined by time-resolved infrared luminescence measurements. *J. Am. Chem. Soc.* **1982,** *104* (20), 5541-5543.

36. Tratnyek, P. G.; Hoigné, J. Oxidation of substituted phenols in the environment: A QSAR analysis of rate constants for reaction with singlet oxygen. *Environ. Sci. Technol.* **1991,** *25* (9), 1596-1604.

37. Haag, W. R.; Hoigné, J.; Gassman, E.; Braun, A. M. Singlet oxygen in surface waters. 1. Furfuryl alcohol as a trapping agent. *Chemosphere* **1984,** *13* (5-6), 631-640.

38. Aeschbacher, M.; Graf, C.; Schwarzenbach, R. P.; Sander, M. Antioxidant properties of humic substances. *Environ. Sci. Technol.* **2012,** *46* (9), 4916-4925.

39. Baciocchi, E.; Bietti, M.; Gerini, M. F.; Lanzalunga, O. Electron-transfer mechanism in the *N*-demethylation of *N*,*N*-dimethylanilines by the phthalimide-*N*-oxyl radical. *J. Org. Chem.* **2005,** *70* (13), 5144-5149.

40. von Sonntag, C.; Schuchmann, H.-P. Peroxyl radicals in aqueous solutions. In *Peroxyl radicals*, Alfassi, Z. B., Ed. John Wiley & Sons: Chichester etc., 1997; pp 173-234.